Influence of Constituents on Thermal Properties of Polymethacrylate Derivatives–Clay Materials

Ruhan Benlikaya,[1] **Mahir Alkan**[2]
[1]*Department of Secondary Science and Mathematics Education, Balikesir University, Balikesir, Turkey*

[2]*Department of Chemistry, Balikesir University, Balikesir, Turkey*

In this study, the solution-mixing method was used to prepare polymethacrylate derivatives' (PaMAs) nanocomposites with kaolinite. It was observed that the resultant materials could include exfoliated, intercalated, and undispersed kaolinite depending on their XRD patterns. TEM micrographs also revealed that platy and tube structures of kaolinite and their stacked form would disperse in the PaMAs. Therefore, they were called PaMAs–kaolinite materials with mixed morphology. The effects caused by different types of PaMA, solvent, and clay (sepiolite and kaolinite) on the thermal properties of these materials were examined. When the thermal stability of the materials was compared on the basis of the functional groups in the PaMAs, it was seen that the materials of the linear PaMAs with kaolinite usually had better thermal stability than that of the ring PaMAs and also seen that the thermal stability of Kao-PaMAs increased from PMMA to poly(ethyl methacrylate) (PEMA) and poly(butyl methacrylate) for linear PaMAs. The solvent type affected the thermal stability and the glass transition temperature of the PaMAs. It was found that THF is the most suitable solvent for increasing thermal stability of the PaMAs in the presence of kaolinite; however, it is difficult to say the same about their T_g temperatures. In addition, the thermal stabilities of PEMA and poly(2-hydroxylethyl methacrylate) were higher in the presence of kaolinite in comparison with sepiolite. The results obtained in this study were explained by the utilization of the relationships among their solubility parameters and of the interactions among the PaMAs, clays, the modifier (octadecylamine) and solvents. POLYM. COMPOS., 32:615–628, 2011. © 2011 Society of Plastics Engineers

INTRODUCTION

Kaolinite, a clay mineral with the 1:1-type layered structure, is a candidate for the host material of nanocomposites due to its high crystallinity and unique structure. One side of its interlayer space is covered with hydroxyl groups of the $Al_2(OH)_4$ octahedral sheets and the other side by oxygen of the SiO_4 tetrahedron [1]. In the kaolinite structure, the strong hydrogen bonding between layers makes the delamination of kaolinite more difficult than that for other platelike silicates such as montmorillonite (MMT) [2]. The apparent scarcity of the studies on kaolinite nanocomposites, especially when compared with MMT, could be due to the fact that the intercalation of kaolinite is very difficult.

To overcome the obstacle mentioned earlier, several techniques have been developed. The most effective of them is the guest displacement reaction, in which preintercalated organic species in kaolinite can be displaced with various types of organic molecules [3]. Various intermediates, such as kaolinite–DMSO [4], kaolinite–MeOH [5], kaolinite–6-aminohexanoic acid [6], kaolinite–dodecylamine [7], kaolinite–KAc [8], kaolinite–GA [9], kaolinite–octadecylamine (ODA) [10], kaolinite–urea [11], and kaolinite–SIM [12], have been used to obtain polymer nanocomposites. Some of the studies are summarized in Table 1 in accordance with the methods used to prepare nanocomposites and with the relevant results [4–13]. In those studies, only PMMA was used in the preparation of polymer nanocomposites as a matrix from polymethacrylate derivatives (PaMAs), and, additionally, the solution-mixing method was used less than the other methods for kaolinite–polymer nanocomposites.

The number of the studies relating to the factors affecting the formation and properties of polymer nanocomposites has significantly increased in the last 10 years, such as those performed on clay morphology [2, 14-17], solvent [18–20], surfactant [21], swelling agent [22], and polymer [14, 23-25]. However, while the studies performed on the clay morphology usually involve the pairs of kaolinite–MMT and sepiolite–MMT, it is a fact that no study has yet been conducted to involve the pair of kaolinite–sepiolite.

In some of the above-mentioned studies, the interactions between polymer and clay [16, 17, 23, 24] were

Correspondence to: Ruhan Benlikaya; e-mail: ruhan@balikesir.edu.tr
Contract grant sponsor: Balikesir University; contract grant number: 2006/01; Contract grant sponsor: TUBITAK; contract grant number: 106T453 (TBAG-HD/186).
DOI 10.1002/pc.21083
Published online in Wiley Online Library (wileyonlinelibrary.com).

TABLE 1. The studies related to kaolinite–polymer nanocomposites.

Method	Intercalation compound	Polymer	Conclusions
In situ polymerization	Kao–dimethylsulfoxide (DMSO)	PVA [4]	
	Kao–dodecylamine	PMMA [7]	Increase in thermal stability [4, 8-10, 12, 13]
	Kao–potassium acetate (KAc)	PMMA [8]	Increase in glass transition temperature [4, 7, 10, 13]
	Kao–glutamic acid (GA)	PBA [9]	Confirming the structure by NMR, XRD and FTIR measurements [5]
	Kao–urea	PMMA [11]	
Solution mixing	Kao–methanol (MeOH)	PVP [5]	The disappearance of glass transition temperature [11]
	Kao–DMSO and Kao–SIM (succunimide)	PVC [12]	The improvements in thermal and optical properties [12]
Melt blending	Kao–6-aminohexanoic acid	Nylon-6 [6]	Increase in thermal stability and glass transition temperature [6, 8, 13]
	Kao-octadecylamine	EVOH [10]	Increase in mechanical properties [10]
	Kao–DMSO	PVC [13]	

used to explain the effects of the mentioned factors on the properties and formation of polymer nanocomposites, while other studies involved the use of the Hildebrand solubility parameters [18, 21, 22, 25] or 3-D Hansen solubility parameters [19, 20] of the pairs of clay-solvent [18], polymer-solvent [18, 19], monomer-solvent [20], surfactant-solvent [21], swelling agent-polymer [22], and polymer-surfactant [25]. According to the Hildebrand solubility-parameter method, the closer the solubility parameters (δ) of the above-mentioned pairs get to each other, the better their miscibility becomes. In the chloroform/methyl ethyl ketone solvent system, where the difference in rubber-solvent and clay-solvent solubility parameter is the lowest, the thermal, mechanical, and optical properties of HNBR–sepiolite nanocomposite are found to be the best [19]. In the 3D Hansen solubility parameter method, the three components of the solubility parameters of polymer/monomer and solvent [i.e., dispersive (δ_d), hydrogen bonding (δ_h), and polar (δ_p)] were used to explain their miscibility. The basal spacing of MMT dispersed in various solvents and monomers was measured by XRD. Their results indicated that the δ_p of monomers and the δ_h of solvents are the main parameters that affect the basal spacing expansion of MMT [20].

It is seen that the factors examined during the study—polymer type, solvent, surfactant (modifier), and clay together—could not be found. Such a study gives us an opportunity to better understand the effects of certain factors on the properties and formation of polymer nanocomposites.

The aim of this work is to examine what types of solvents, clays, and functional groups in the polymers affect thermal properties of the resultant PaMAs materials and to explain the obtained results through utilization of the relationships among their solubility parameters and of the probable interactions among PaMAs, the modifier (ODA), clays, and solvents. Therefore, PMMA, poly(ethyl methacrylate) (PEMA), poly(2-hydroxylethyl methacrylate) (PHEMA), poly(butyl methacrylate) (PBMA), poly(isobornyl methacrylate) (PIBOMA), poly(benzyl methacrylate) (PBzMA), poly(cyclohexyl methacrylate) (PCHMA), and the structures of which are given in Fig. 1 were used to prepare their nanocomposites with kaolinite by the solution-mixing method. The thermal properties of PEMA and PHEMA products with kaolinite were compared to those of the nanocomposites with sepiolite [24] to examine the effect of the clay type.

EXPERIMENTAL

Materials

All the chemicals used in this study were of analytical grade and used without further purification. PMMA, PEMA, and PCHMA were obtained commercially from Across. PHEMA, PBMA, PIBOMA, and PBzMA were provided from Aldrich. The kaolinite sample was supplied from Kalemaden Corporation (Turkey). The XRD pattern of kaolinite sample (JCPDS 29-1488) is shown in Fig. 2. The sample also includes muscovite and quartz as shown in the previous study [26].

Modification of Kaolinite

The kaolinite sample was oven-dried, ground, and sieved to a size of 50 μm diameter. Then, the clay was modified with ODA by passing through two precursors, Kao–NMF (*N*-methyl formamide) and Kao–NMF–MeOH, according to the synthesis route described in a previous work [27]. The study found that when the methanol-treated kaolinite–NMF intercalation compound was used as the intermediate, alkyl amines were intercalated into the interlayer space of kaolinite.

Preparation of Nanocomposites

The solution-mixing method involves dispersion of the filler in an organic solvent followed by dissolution of the polymer matrix and solvent casting. The method brings better dispersion of nanoparticles compared to the other methods [28, 29], as Choudhury et al. [19] stated. The challenge in this method is to find the best solvent, because interactions among polymer, filler, and solvent play an important role on the properties of nanocomposites. Table 2 summarizes the procedure followed in this

 DOI 10.1002/pc

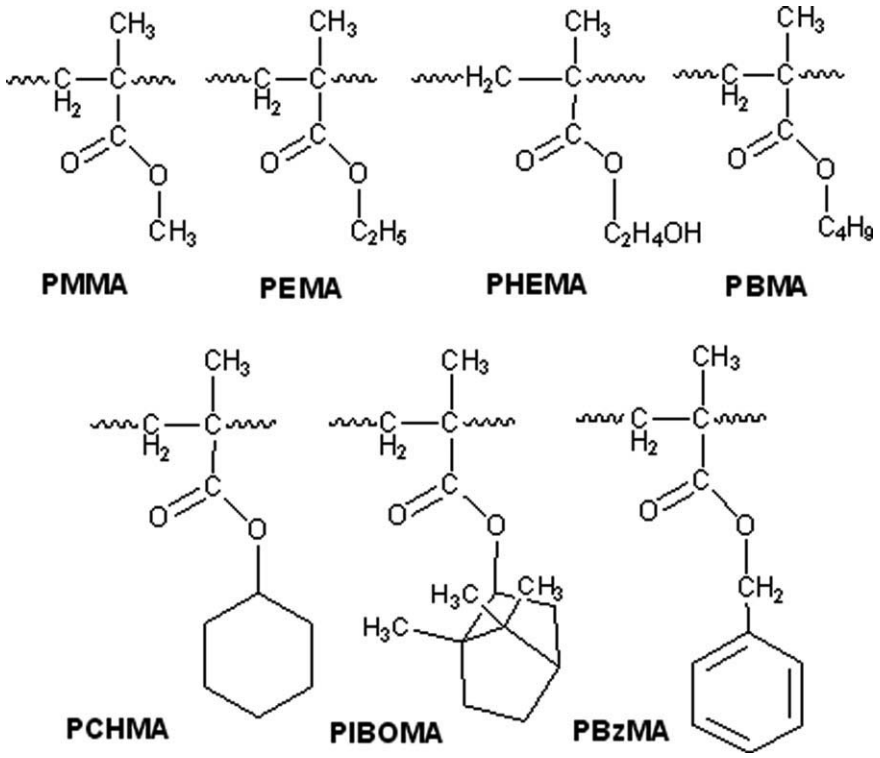

FIG. 1. PaMAs used in the study.

work. The samples were prepared in concentrations of 2.5% of the filler. The obtained products were identified as Kao–PMMA, Kao–PEMA, etc.

The filler was suspended in the solvents/mixtures by ultrasonic treatment. The polymer was added to the suspensions, and they were then subjected to magnetic stirring for 24 h. The mixtures were subsequently poured into a glass petri dish and dried at 40°C for 2 days to remove any residual solvent.

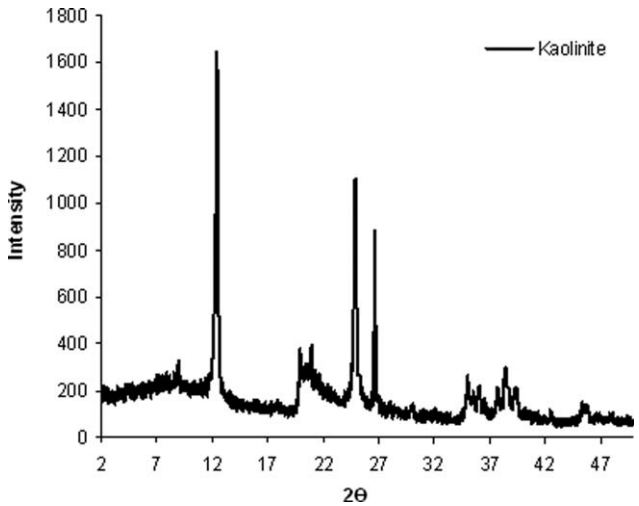

FIG. 2. XRD pattern of kaolinite.

Characterization Techniques

XRD patterns were obtained using Panalytical Pro MPD. The X-ray beam was derived from nickel-filtered Cu Kα ($\lambda = 0.154$ nm) radiation in a sealed tube operated at 40 kV, 30 mA, and the diffraction curves ranged from 2° to 50° at a scan rate of 0.02°/min. SEM observations were carried out with FEI QUANTA 200 F at 5 kV, placing film samples onto a carbon film. The TEM micrographs were obtained with JEM 2100//JEOL at an acceleration voltage of 100 kV. For TEM study, the samples were ultramicrotomed with a diamond knife on FIA Leica EM UC6 microtome at room temperature to give 60–80 nm thick sections. The sections were collected on 200-mesh Lacey carbon film-coated copper grids.

TABLE 2. The procedure followed in this study.

Polymer	Filler	Solvent
PMMA	Kaolinite	DCM, THF
PEMA	Kaolinite, sepiolite	DEE:EtOH (1:1), THF[a]
PHEMA	Kaolinite, sepiolite	EtOH, EtOH:THF (1:4)[a]
PBMA	Kaolinite	DCM, THF
PCHMA	Kaolinite	DCM, THF
PIBOMA	Kaolinite	DCM, THF
PBzMA	Kaolinite	DCM, THF

[a] The samples were prepared for this study to provide contribution to examination of solvent effect in the presence of sepiolite.

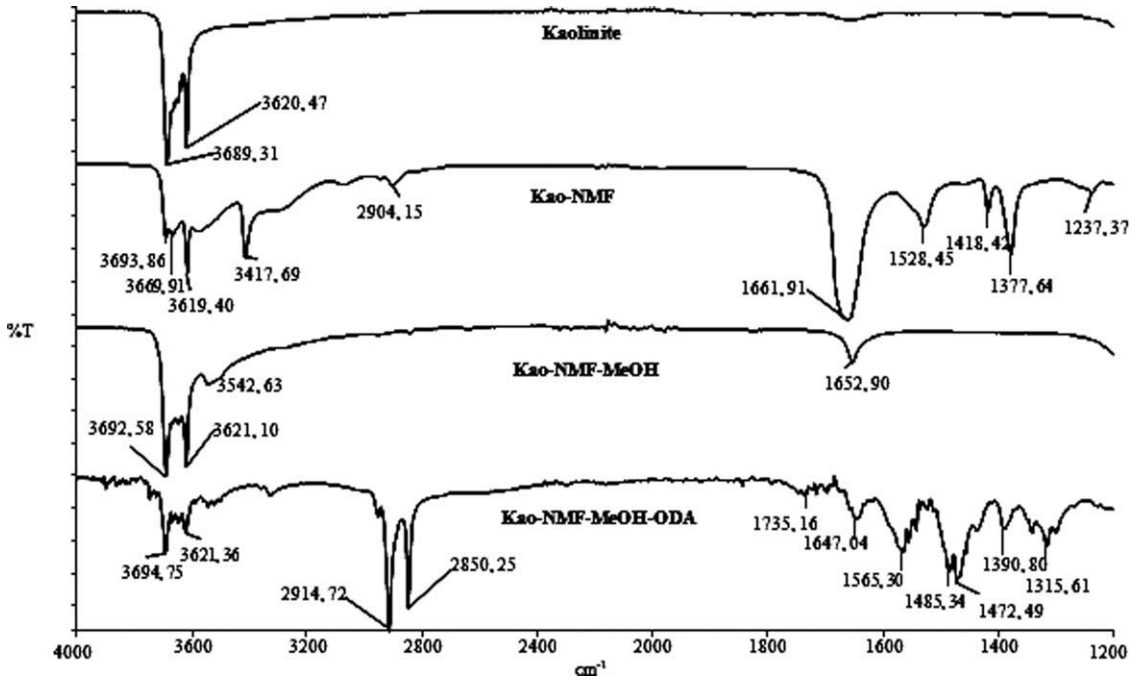

FIG. 3. FTIR spectra of kaolinite, Kao–NMF, Kao–NMF–MeOH, and Kao–NMF–MeOH–ODA.

The thermal stability of the PaMA materials was examined using a Perkin Elmer Pyris Diamond TG/DTA. The TG scans were recorded at a temperature ramp of 10°C/min under a constant nitrogen flow of 200 ml/min from 50 to 600°C. DTG curves and FTIR spectra of residue samples at various temperatures determined according to DTG curves were used to investigate if a change occurred in thermal degradation mechanism of the PaMAs. Glass transition temperatures were investigated at a temperature ramp of 20°C/min in nitrogen flow by Perkin Elmer Sapphire DSC. The temperatures were determined as the midpoints of reverse "S"-shaped thermograms.

RESULTS AND DISCUSSION

Modification of Kaolinite

FTIR Measurements. The kaolinite sample was characterized by a diagnostic, signature O—H stretching pattern consisting of four bands at 3689, 3669, 3653, and 3621 cm^{-1} as can be seen in Fig. 3. Because the last band at 3621 cm^{-1} was assigned to the stretching frequency of the internal hydroxyl group of kaolinite, which is oriented almost parallel to the direction of the (00l) layers, this band was not usually influenced very much by inter lamellar modification reactions. On the other hand, the inner surface hydroxyl groups associated with the remaining bands (3,689, 3,669, and 3,653 cm^{-1}) are believed to make an angle of 60°–73° with the [001] plane of kaolinite [30]. They were thus very much influenced by interlamellar modifications.

In the FTIR spectrum of the Kaolinite–NMF intercalation compound, the peaks due to the carbonyl stretching at 1,662 cm^{-1}, C—H stretching 2,904 cm^{-1}, and N—H stretching at 3,417 cm^{-1}, and the broad bands at around 3580 and 3290 cm^{-1} related to hydrogen bonded —OH and —NH groups appeared. The peak at 3,689 cm^{-1} in kaolinite was shifted to a lower wavelength. For the treatment of kaolinite–NMF by MeOH, the new peak was observed at around 1,653 cm^{-1}. The peak was assigned to H—O—H bending, indicating that some amount of water was present in the methanol-treated kaolinite [31]. The band at around 3,543 cm^{-1} was characteristic for hydrated kaolinite, indicating that the hydrogen bonds between OH groups of kaolinite and water molecules are present. In the spectrum of Kao–NMF–MeOH–ODA, the decrease was observed in the intensity of the hydroxyl stretching bands of kaolinite. The new peaks at two regions, 3,200–3,800 cm^{-1} and 1,200–1,600 cm^{-1}, and the shift in the peak at 3,695 cm^{-1} possibly occurred by the treatment of ODA into Kao–NMF appeared. The fact that FTIR spectra of Kao–NMF–MeOH and Kao–NMF–MeOH–ODA are not same shows that the intercalation compound in this study is different from Kao–NMF–MeOH.

XRD Patterns. Figure 4 shows X-ray diffraction (XRD) patterns of Kao–NMF, Kao–NMF–MeOH, and Kao–NMF–MeOH–ODA. When the gallery space of kaolinite was intercalated by NMF, the position of the 001 peak changed from $2\theta = 12.4°$ (see Fig. 2) to $2\theta = 8.3°$. The result shows that Kao–NMF intercalation compound was formed. In the case of Kao–NMF–MeOH–ODA, it is clear that the peaks at 10.3 and 8.4° observed in its XRD pattern belong to dried Kao–NMF–MeOH and Kao–NMF,

 DOI 10.1002/pc

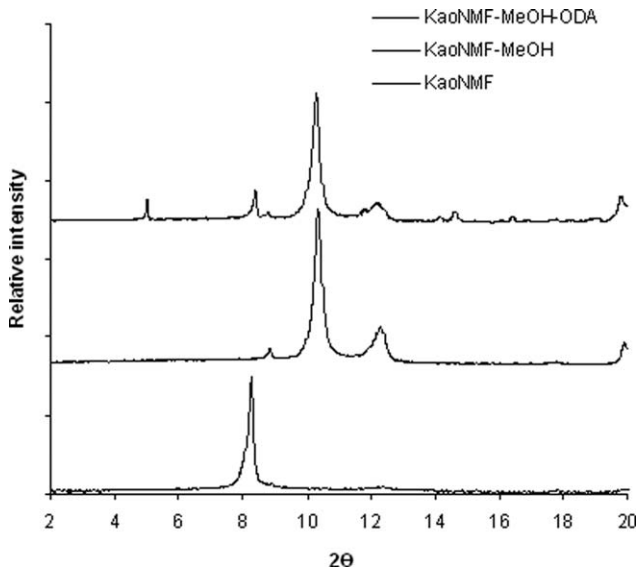

FIG. 4. XRD patterns of Kaolinite, Kao–NMF, Kao–NMF–MeOH, and Kao–NMF–MeOH–ODA.

respectively in Fig. 4. In addition, the peak at $2\theta = \sim 5^\circ$ possibly showed the presence of ODA in kaolinite structure. The findings point out that intercalated NMF molecules do not completely displace the ODA molecules in MeOH. The observed peak with very low intensity at 12.4° belonging to kaolinite shows that intercalation could not be completed. Hence, the product consisting of a mixture of mainly Kao–NMF–MeOH and Kao–NMF–MeOH–ODA was called as Kao–Int.

PaMA Nanocomposites

XRD Patterns. In XRD patterns of the Kao–PaMAs materials, three peaks (≈8.4°, 10.5°, and 12.6°) were observed, and the peak at ~5°, which formed by ODA treatment, disappeared as seen in Fig. 5a–d. The first peak at 8.4° was seen in XRD patterns of Kao–PEMA (THF) and Kao–PBMA (DCM) materials (Fig. 5a and b). The finding shows new intercalated structures formed between the polymers and kaolinite.

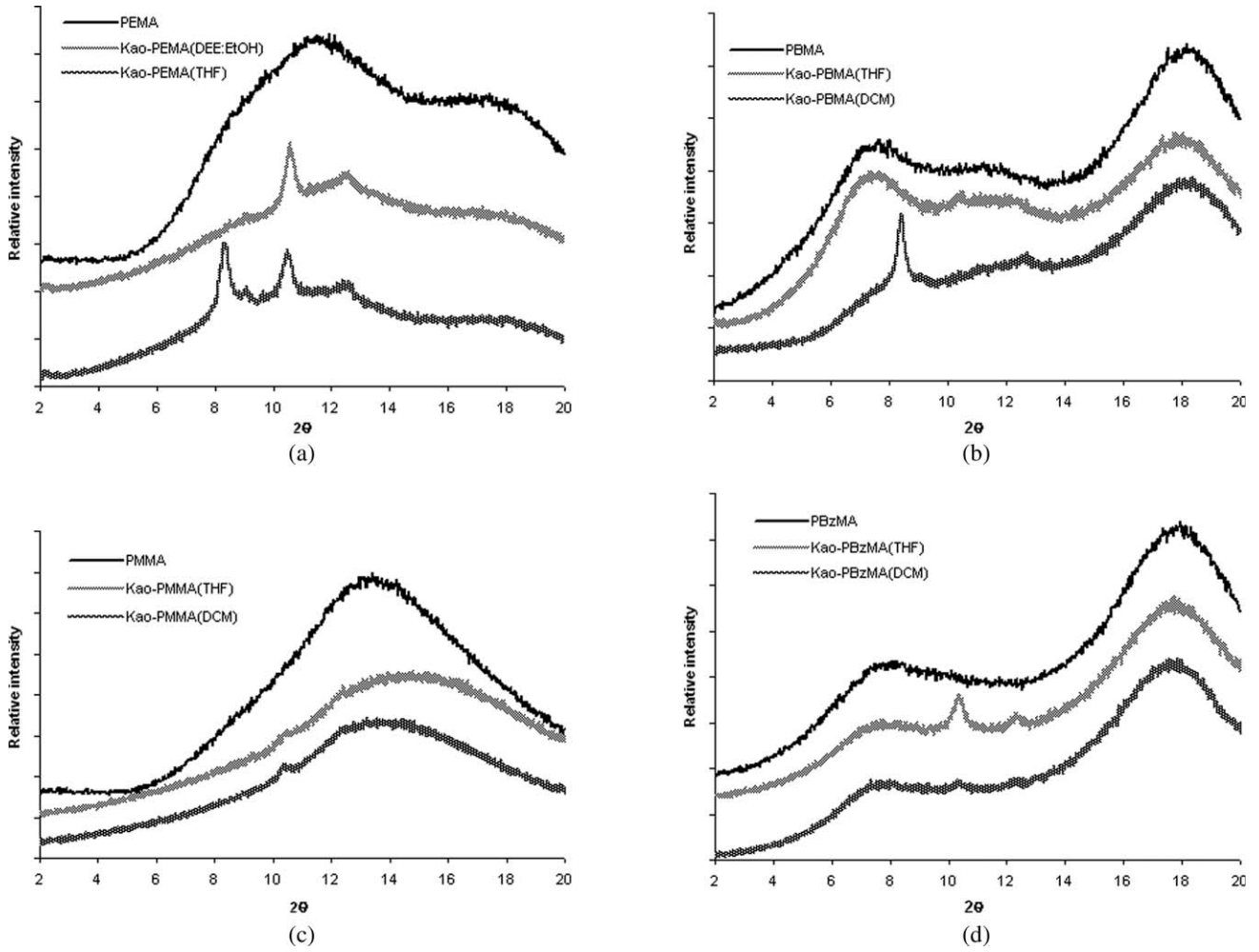

FIG. 5. (a) XRD patterns of PEMA and Kao–PEMAs; (b) XRD patterns of PBMA and Kao–PBMAs; (c) XRD patterns of PMMA and Kao–PMMAs; (d) XRD patterns of PBzMA and Kao–PBzMAs.

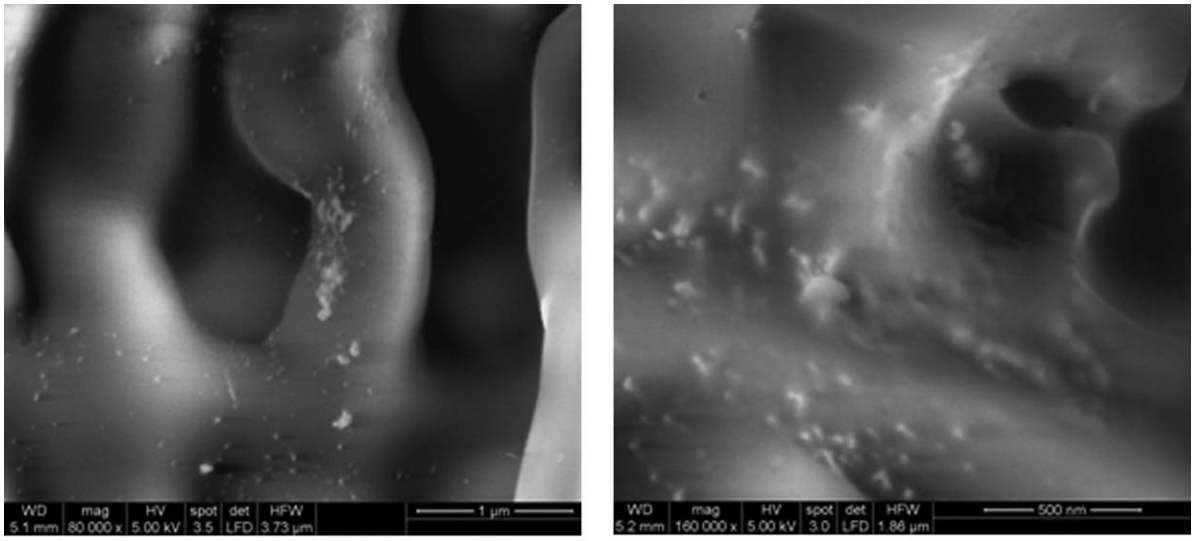

(a) (b)

FIG. 6. (a, b) Sample SEM images of Kao–PaMAs.

Kao–PMMAs and Kao–PEMAs have the second peak at $\sim 10.5^{\circ}$ as shown in Fig. 5a and c. This result shows that Kao–Int compound could not interact with the polymers sufficiently to disperse in them. PHEMA, PCHMA, and PIBOMA materials with kaolinite also show similar behavior to the PMMA materials. In addition, it was seen in Fig. 5b and d that Kao–PBMA (THF) and Kao–PBzMA (DCM) materials did not have the two mentioned peaks and Kao–PBzMA (THF) had the second peak at 10.5°. These findings relating to PEMA, PBMA and PBzMA show that solvent medium affects the dispersion degree of Kao–Int in the polymers. However, it was concluded that THF usually provides better dispersion of kaolinite in the PaMAs.

The third peak with a very low intensity at 12.6° was observed in most of the products. This peak arises from undispersed kaolinite in the Kao–Int compound as mentioned before.

Morphological Analysis. Figure 6a and b presents the SEM sample images of Kao–PaMAs. The images show that kaolinite plates were embedded in PaMAs.

Figure 7a–c shows the sample TEM images of the resulting materials. On the basis of the analysis of the images, it is determined that the dark particles belong to the kaolinite, and light area is related to the PaMAs. The images reveal that platy and tubular structures of kaolinite particles and their stacked form dispersed in the PaMA samples.

Thermal Stability. Thermal stabilities of the samples were investigated by considering the degradation temperatures at 10, 30, 50, and 80% weight losses. The data obtained from TG curves of the PaMAs and their materials with Kao–Int are given in Table 3. The table shows that the incorporation of kaolinite into the PaMAs usually enhances thermal stability of the PaMAs. However, a decrease in T_{10} temperatures of PMMA and PHEMA materials was observed. The decrease in PMMA was more significant than PHEMA.

In another study [11] of PMMA nanocomposites shown in Table 1, the improvement in thermal stability of PMMA was observed in the temperature range of 250–550°C, and the onset of degradation was not influenced, although the XRD pattern of the nanocomposites has no reflection pertaining to the presence of any remaining ordering of kaolinite. In the presence of Kao–Int, the T_{10} temperature of PMMA decreased considerably as shown in Table 3, although the intensity of Kao–Int was very low in XRD pattern of Kao–PMMAs.

Compared to the solvent mediums shown in Table 2, the thermal stabilities of the PaMA materials with kaolinite were usually found to be the best in THF solvent/mixtures. In this medium, the highest increase in thermal stability was observed for Kao–PEMAs and Kao–PBMAs, while the thermal stability of Kao–PMMAs did not change noticeably by using different solvents. On the other hand, the interaction among PaMA, THF, and kaolinite was getting better as it occurred from PMMA to PEMA and PBMA. Among the materials of the ring PaMAs, Kao–PIBOMA had the highest increase in thermal stability in THF medium.

When the thermal stability of the materials was compared according to the functional groups in the PaMAs, it was seen that the composites of the linear PaMAs usually had better thermal stability than those of the ring PaMAs. This could result from the fact that the bulky ester groups in the ring PaMAs cause the steric effect and that this effect hampers the interaction between COO^{-} group in the PaMAs and Kao–Int.

Considering TG data of PEMA/PHEMA materials with sepiolite and kaolinite, the thermal stability of Kao–PEMA (THF) is better than Sep–PEMA (THF). For this reason, we can say that, in the PaMAs, THF solvent facil-

 DOI 10.1002/pc

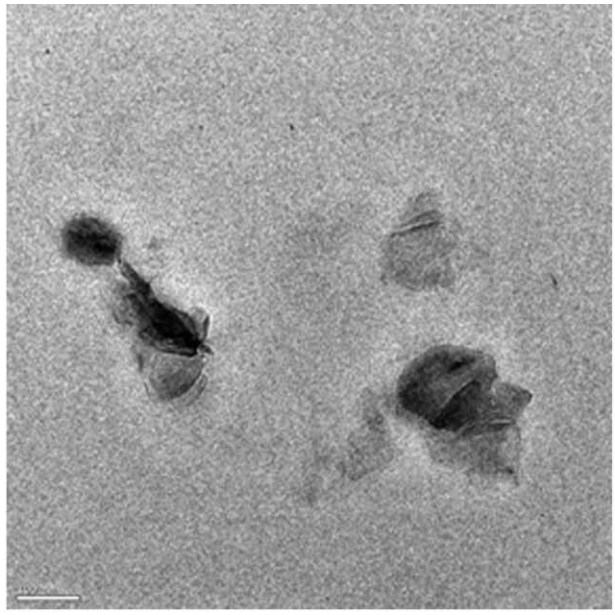

(a)

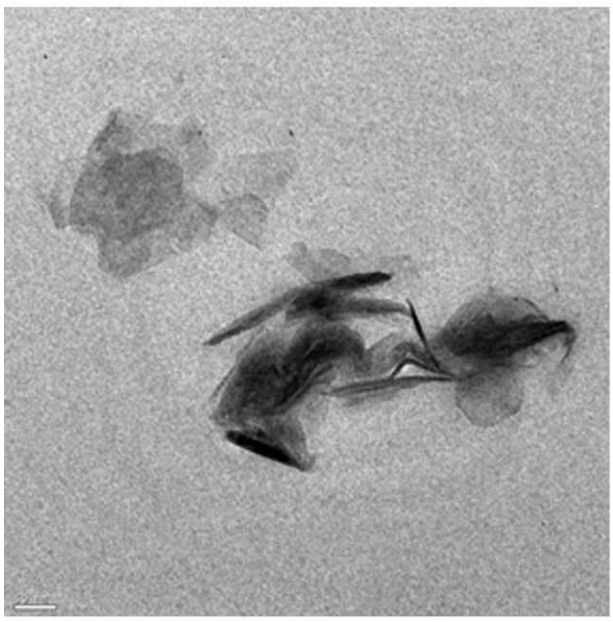

(b)

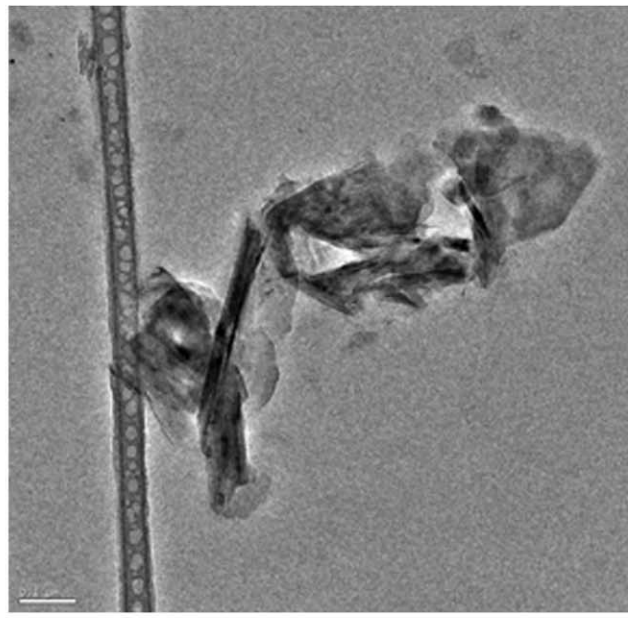

(c)

FIG. 7. (a–c) Sample TEM images of Kao–PaMAs.

itates the dispersion of kaolinite better than sepiolite. Becasue T_{10} and T_{30} temperatures of the material with sepiolite prepared in DEE:EtOH were higher than that of kaolinite, the DEE:EtOH mixture was thought to be more convenient for sepiolite–PEMA materials. In addition, it was observed that the thermal stability of PHEMA materials with kaolinite was better than that of sepiolite and that EtOH:THF mixture caused better dispersion of kaolinite in PHEMA. The differences observed for these materials arise from interactions among the clays, solvent mediums, and the PaMAs.

The structure of clay used in preparing the polymer nanocomposites influences their thermal properties. In general, it was concluded that kaolinite is more effective than sepiolite to improve the thermal properties of the PaMAs. The reason why sepiolite-filled Nylon-6 (N6) nanocomposites exhibited better properties when compared with N6 materials with MMT could be explained with the fact that the nanodisperison of sepiolite in N6 matrix is caused by the strong interaction of the N6 chains with the Si—OH groups on sepiolite, together with the high shear stresses during compounding that tends to

TABLE 3. The data obtained from TG and DSC curves of the PaMAs and their materials with kaolinite/sepiolite.

System	T_{10}[a] (°C)	T_{30}	T_{50}	T_{80}	T_g[b]
PMMA	347	369	380	397	110
Kao–PMMA (DCM)	303	370	382	399	143
Kao–PMMA (THF)	205	368	381	398	126
PEMA	236	272	303	356	64
Kao–PEMA (DEE:EtOH)	261	297	347	391	71
Kao–PEMA (THF)	310	373	394	432	62
Sep–PEMA (DEE:EtOH)	276	309	349	386	70
Sep–PEMA (THF)	209	279	319	359	52
PHEMA	303	345	365	402	92
Kao–PHEMA (EtOH)	299	353	378	416	90
Kao–PHEMA (EtOH:THF)	304	361	387	424	86
Sep–PHEMA (EtOH)	301	346	371	415	90
Sep–PHEMA (EtOH: THF)	250	342	370	398	78
PBMA	236	281	305	342	26
Kao–PBMA (DCM)	273	315	352	393	27
Kao–PBMA (THF)	299	358	386	417	29
PCHMA	274	299	323	382	108
Kao–PCHMA (DCM)	280	306	339	423	106
Kao–PCHMA (THF)	298	338	351	437	138
PIBOMA	224	252	277	318	109
Kao–PIBOMA (DCM)	249	284	312	409	115
Kao–PIBOMA (THF)	240	310	317	435	97
PBzMA	272	307	346	370	69
Kao–PBzMA (THF)	281	316	341	367	67
Kao–PBzMA (DCM)	290	334	353	376	54

[a] The temperature for 10% weight loss.
[b] Glass transition temperature.

destroy agglomerated structures [15]. In an earlier study of Bokobza, it was concluded that while the lack of interfacial adhesion between PDMS and MMT causes slight reinforcement, the interactions between the —OH groups existing along sepiolite and the PDMS chains are responsible for the extent of reinforcement imported by these nanofibers [16].

In this study, the obtained results can be interpreted by considering the differences in the interactions between the PaMAs and the fillers and then by comparing them to the literature. The following explanations can be used to understand the observed differences caused by fillers and solvents in TG results of the PaMA materials.

Sepiolite's surface is covered with silanol groups (Si—OH) spaced every 5 Å along the fiber edges while, in case of the structure of kaolinite like MMT, the broken Si—O—Si bonds of the terminal silica tetrahedral lead to the formation of silanol groups [32].

Although kaolinite is composed of highly perfect small platelets (0.2–2 μm) of ~80 nm thickness [33], sepiolite consists of the fibers that are 10–5,000-nm long, 10–30 nm wide, and 5–10 nm thick [34]. Hence, the surface areas of kaolinite and sepiolite interacting with the PaMAs and the aspect ratios (width/length) of them are different.

The attraction forces holding sepiolite fibers/fiber bundles together must be overcome to disperse sepiolite in the PaMAs. However, in PaMAs' materials with kaolinite, the solvent and PaMAs chains must exchange intercalating agents (NMF, MeOH, etc.) in Kao–Int compound. The formed interactions need stronger than hydrogen bonding between kaolinite and intercalating agent.

In addition to the above, the thermal stability of the materials changes depending on the solvents, because they can affect the dispersion of clay in polymer. For instance, using THF usually improves thermal stability of the PaMAs. The reason for this could be that THF is cyclic ether and thus has an oxygen atom with unpaired electrons, which can facilitate the interacton between the PaMAs and these clays.

DSC Measurements. Table 3 also includes glass transition temperatures (T_g) obtained from DSC curves of the PaMA materials. Although an increase in T_g temperatures was observed for Kao–PMMAs, Kao–PEMA(DEE:EtOH), Kao–PBMA(THF), Kao–PCHMA(THF), and Kao–PIBOMA(DCM), a decrease was seen for other products. These findings reveal that the type of solvent affects the T_g temperatures of Kao–PaMAs. The increases are tentatively attributed to the confinement of the PaMAs chains when interacted with the clay galleries that prevents the segmental motions of the polymer chains.

Although the thermal stability of PMMA did not change significantly in the presence of kaolinite after T_{30}, an increase was observed in its T_g temperature. In another study [7] of PMMA nanocomposites shown in Table 1, Kao–dodecylamine also increased T_g temperature of PMMA.

Compared to the T_g temperatures of sepiolite and kaolinite materials with PEMA/PHEMA, it was seen that while THF or its mixture caused a greater decrease in their T_g temperatures, no significant difference was observed for DEE:EtOH and EtOH mediums in the case of different clay types.

Solubility Parameters and Thermal Properties

On the basis of the concept of cohesive energy that is associated with the net attractive interactions of the material, Hildebrand and Scott proposed the definition of what is generally called the solubility parameter: $\delta_t = (E/V)^{1/2}$, where E shows molar cohesive energy and V is the molar volume [21]. Hansen extended the Hildebrand parameter to three components: the dispersive component (δ_d), the polar component (δ_p), and hydrogen-bonding component (δ_h). The equation is expressed as $\delta_t^2 = \delta_d^2 + \delta_p^2 + \delta_h^2$ [20]. Although it may be preferable to use Hansen's solubility parameters for the polymers used in polymer/clay/surfactant system when considering interaction between polymer/surfactant and polymer/clay, there are not enough and consistent data for the Hansen's solubility parameters of the polymers of interest in the literature [25].

The Hansen/Hildebrand solubility parameters [35–40] found for the PaMAs and solvents are summarized in Table 4. The results obtained in this study were explained by using the relationships among their solu-

DOI 10.1002/pc

TABLE 4. Hansen/Hildebrand solubility parameters of used solvents and PaMAs.

Sample	Solubility parameters $(MPa)^{1/2}$			
	δ_d	δ_p	δ_h	δ_t
Polymers				
PMMA (R: 8.6)	18.6	10.5	7.5	22.6
PEMA (R: 10.6)	17.6	9.6	2.5	20.2
PHEMA	15.1	11.9	18.8	26.9
PBMA	18.0	8.4	3.1	20.1
PBzMA	–[a]	–[a]	–[a]	20.1
PIBOMA	–[a]	–[a]	–[a]	16.9
PCHMA	–[a]	–[a]	–[a]	18.8
Solvents				
THF	16.8	5.7	8.0	19.5
EtOH	15.8	8.8	19.4	26.5
DCM	18.2	6.3	5.9	20.1
DEE	14.5	2.9	5.1	15.6

[a] The data not been found in the literature.

bility parameters of the groups of ODA-solvents, KaoInt–PaMAs, PaMAs-solvents, and PaMAs–KaoInt/sepiolite-solvents.

ODA-Solvents and KaoInt-PaMAs. A similar approach to the study of Ho and Glinka [21] can be used if it is assumed that Kao–Int involves only ODA. The solubility parameter for ODA (δ_{ODA}) was given 19.5 $MPa^{1/2}$ [41]. The fact that δ_{ODA} is the same as the solubility parameter of THF given in Table 4 could partially explain that KaoInt–PaMA materials prepared in THF medium usually have better thermal stability independently from PaMA type. They took into consideration only the solubility parameter of the modifier instead of modified MMT in their study. The change that modification caused on the solubility parameter of clay can also be important for explaining the findings in this study. Although it is not possible to obtain the solubility parameter of natural clay, it can be considered to be a highly polar material due to the presence of negative superficial charges on the structure. This polar character confers a high solubility parameter to the clay [42]. ODA surface treatments lead to a significant decrease in polar and hydrogen-bonding components of Hansen parameter of silica fumes, dispersion force component slightly increases [43]. The similar change could also be valid for the modification of kaolinite with ODA. The reason why Kao–Int dispersed better in PEMA/PBMA in THF medium compared to PMMA and PHEMA, which have higher hydrogen and polar components of solubility parameter than the others, could be explained with the change in the components of solubility parameter of kaolinite after modification with ODA.

PaMAs-Solvents and PaMAs-KaoInt/Sepiolite-Solvents. To explain the obtained findings for linear PaMAs, the solubility parameters in Table 4 were translated to the triangular graph using a set of fractional parameters, f_d ($\delta_d/\delta_d + \delta_p + \delta_h$), f_p ($\delta_p/\delta_d + \delta_p + \delta_h$) and f_h ($\delta_h/\delta_d + \delta_p + \delta_h$) as can be seen in Fig. 8. Such a triangular graph was used to investigate the influence of organic solvents with different polarity on properties of PMMA/MWNT composites [44].

It can be clearly seen in Fig. 8 that while f_d increases from PMMA to PBMA, f_h decreases. Compared to the thermal stabilities of Kao–PaMAs (THF) and the change in f_d and f_h of lineer PaMAs, higher f_d and lower f_h force of the PaMAs facilitates dispersion of Kao–Int in them and causes better thermal stability of the Kao–PaMAs materials. As to their T_g temperatures, Kao–Int could increase more in T_g of PaMAs with a lower f_d and higher f_h. For the ring PaMAs, such a comparison could not be made due to insufficient data.

The three fractional parameters of EtOH are very close to PHEMA, when that of THF:EtOH mixture can be further than PHEMA compared to EtOH as in Fig. 8. Hence, it can be thought that EtOH is a better solvent for PHEMA. Although the fact that Kao–PHEMA prepared in the mixture has better thermal stability is in conflict with the result, Sep–PHEMA (EtOH) with better thermal stability supports the result. Sepiolite can probably have higher δh compared to kaolinite due to its surface covered with silanol groups (Si—OH) spaced every 5 Å along the fiber edges [32], while modification of kaolinite with ODA leads to a decrease in polarity of kaolinite. Kao–PBMA (THF) has better thermal stability, despite the fact that f_d, f_h, and f_p parameters of DCM are closer to that of PBMA compared to the parameters of THF. It shows that Kao–Int is dispersed well by a solvent with lower f_d and higher f_h in PBMA.

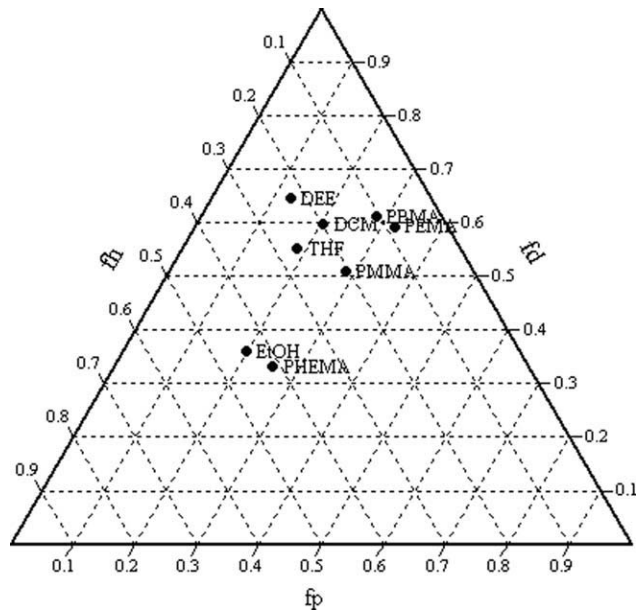

FIG. 8. The triangular graph of dispersion, polar, and hydrogen bonding fractional solubility parameter, f_d, f_p, and f_h of used linear PaMAs and solvents.

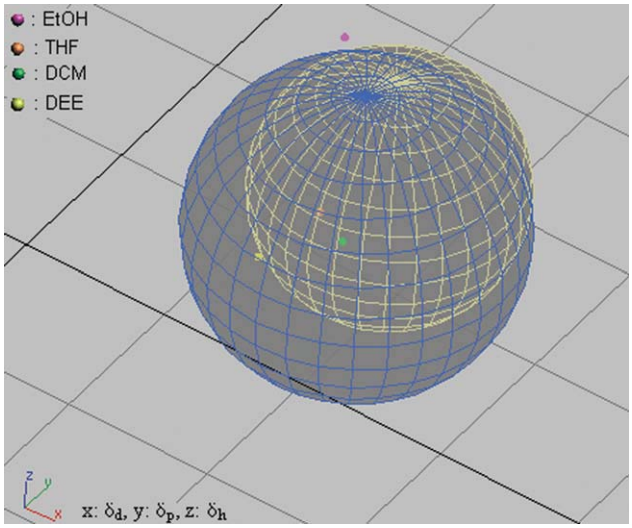

FIG. 9. Hansen solubility spheres of PMMA and PEMA. [Color figure can be viewed in the online issue, which is available at wileyonlinelibrary.com.]

In the case of the ring PaMAs, it is seen that the solubility parameters of DCM and THF are closer to that of PBzMA ($\delta_{diff(THF)} = 0.6$ and $\delta_{diff(DCM)} = 0$) and PCHMA ($\delta_{diff(THF)} = 0.7$ and $\delta_{diff(DCM)} = 1.3$) than that of PIBOMA ($\delta_{diff(THF)} = 2.6$ and $\delta_{diff(DCM)} = 3.2$). Although $\delta_{diff\ (THF,\ DCM)}$ values for PBzMA and PCHMA are lower than that of PIBOMA, Kao–PIBOMAs have better thermal stability than Kao–PBzMAs and Kao–PCHMAs. Owing to the fact that the polymers with aromatic rings all show rather restricted solubility ranges, Kao–PBzMA could have less thermal stability. Hughes and Britt [45] found that no common alcohols were found to attack high molecular weight PS or PBzMA, although alcohols with $\delta = 9.5$–10.5 ($cal^{1/2}$ $cm^{3/2}$) do dissolve PIBOMA. These results show that using the Hildebrand solubility parameter, without three components to explain, the compatibility for the groups of PaMAs-solvent and PaMA–KaoInt-solvents is not sufficient. If 3D solubility parameters of the PaMAs could be found, it would be possible to offer a more accurate explanation for the difference in thermal properties of the linear PaMA materials and the ring PaMA materials.

PMMA/PEMA–KaoInt/Sepiolite-Solvents. The Hansen solubility spheres only for poly(methyl methacrylate) (smaller circle, *R*: 8.6) and poly(ethyl methacrylate) (larger circle, *R*: 10.6) are shown in Fig. 9, as radius values of solubility spheres for other PaMAs have not been found. A polymer is probably soluble in a solvent (or solvent blend) if the Hansen parameters of the solvent lies within the solubility sphere for the polymer [36]. Although THF inside the solubility spheres of PMMA and PEMA is a good solvent for both of them, the fact that Kao–PEMA has better thermal stability shows that Kao–Int could disperse better in them as the values of f_h components of PaMAs reduce. In addition, although DEE:EtOH (1:1) mixture is also probably inside the solubility sphere of PEMA, the fact that Kao–PEMA in THF have better thermal stability than Kao–PEMA (DEE:EtOH) shows that Kao–Int better disperses a solvent with less f_h.

Taking into account the change in T_g temperatures of the PaMAs, Kao–Int restricts the mobility of polymer segments with higher δ_d well in the PaMA materials prepared in THF medium. When the obtained results for Kao–PaMAs prepared in various solvents/mixture were compared, it was seen that while the solvent (DCM) with higher f_d and lower f_h caused more increase in T_g temperature of Kao–PMMA, Kao–PEMA prepared in the mixture (DEE:EtOH) with higher f_h had better T_g temperature.

A comparison of the thermal properties of Kao–PEMAs to those of Sep–PEMAs shows that the type of filler can change the thermal properties of PEMA materials prepared in the same solvent. The fact that sepiolite can probably have higher δh compared to Kao–Int means that DEE:EtOH with higher δh compared to THF causes higher thermal stability for Sep–PEMA.

DTG Curves. Thermal degradation of poly-*n*-alkyl methacrylates produces monomers as a result of depolymerization, which is the main reaction in this degradation process. The formation of poly(methacrylic acid) (PMA) and its decomposition in which various poly(methacrylic anhydride)s (PMAn) occur are also usually a characteristic process in PaMAs' thermal degradation at high temperature except poly(methyl methacrylate). The degradation products are of low molecular weight, and their composition depends on the chemical structure of the side chain of the polymer [24, 46, 47].

For the DTG curves of PMMA and PBzMA did not change in the presence of kaolinite, the DTG curves of the other PaMAs materials were given in Fig. 10a–e. In the case of PEMA nanocomposites with sepiolite in previous study [24], the shift in the right shoulder in the DTG curve of PEMA to a higher temperature and the broadening in the peak related to the formation of anhydride structure were also observed in the DTG curves of PEMA materials with kaolinite, as can be seen from Fig. 10a. However, the first degradation step between 150 and 300°C almost disappeared in Kao–PEMA (THF), and the second right shoulder in PEMA between 410 and 460°C was seen as a small peak in both of the Kao–PEMA materials.

The distinct peak at around 420°C, which was not observed in DTG curve of PHEMA, was identified in that of Kao–PHEMA nanocomposites in Fig. 10b. The same change had been observed for PHEMA materials with sepiolite [24].

The DTG curves of Kao–PBMAs have several small peaks between 250 and 400°C and a shift of main degradation peak of PBMA, while it degrades in one step (Fig. 10c). Some similarities in the DTG curves of Kao–PCHMA and Kao–PIBOMA were observed as can be seen in Fig. 10d and e: the peak between 200 and 300°C was shifted to higher temperatures for the materials pre-

 DOI 10.1002/pc

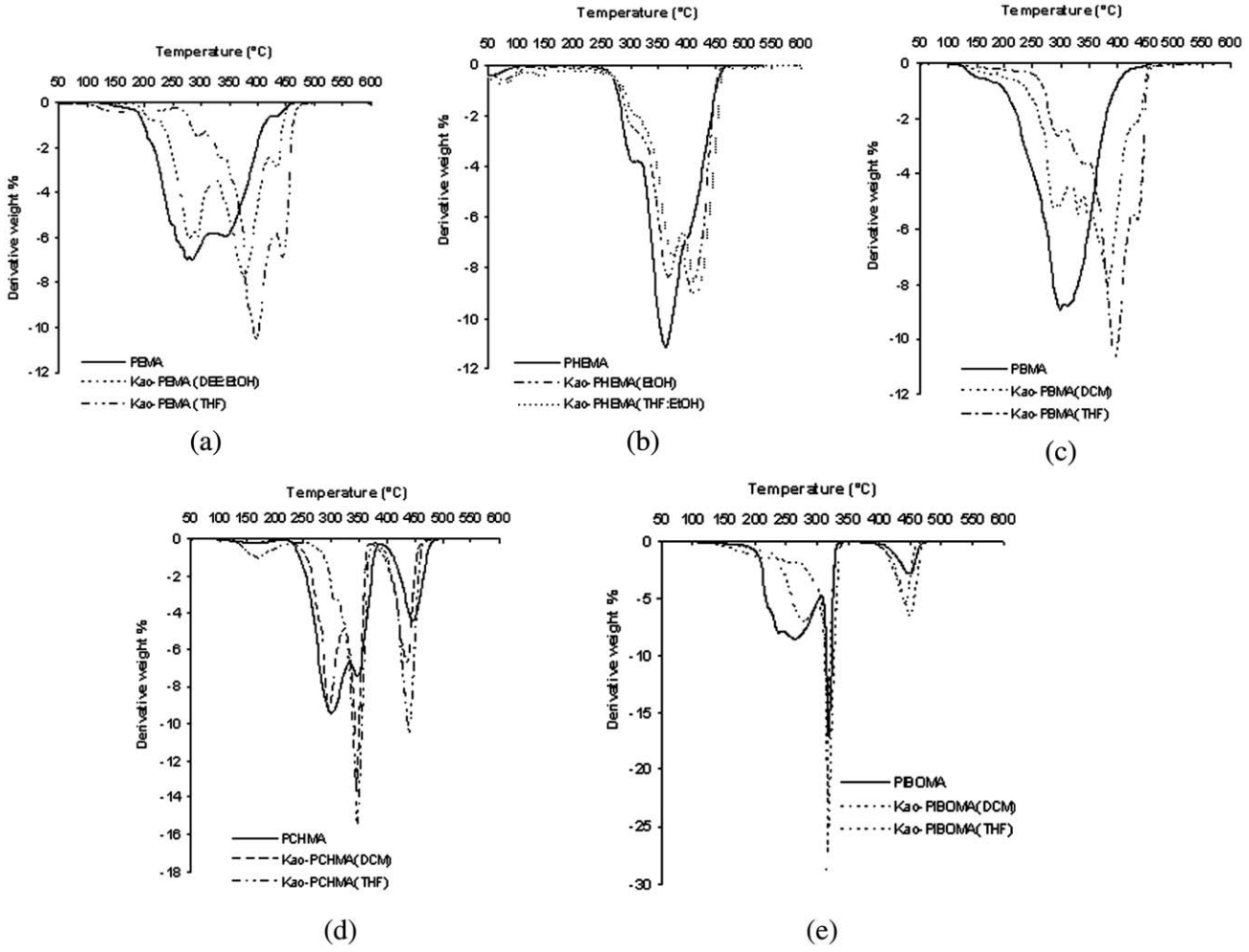

FIG. 10. (a) DTG curves of PEMA and Kao–PEMAs; (b) DTG curves of PHEMA and Kao–PHEMAs; (c) DTG curves of PBMA and Kao–PBMAs; (d) DTG curves of PCHMA and Kao–PCHMAs; **(e)** DTG curves of PIBOMA and Kao–PIBOMAs.

pared in DCM while the peak nearly disappeared for that of THF. However, the peak between 400 and 500°C was shifted to a lower temperature in Kao–PCHMAs.

The infrared spectra of residues at various temperatures were studied to understand the observed differences in the DTG curves for PEMA, PBMA, PCHMA, and PIBOMA, which are shown in Fig. 11a–c. Compared to the FTIR spectra of PEMA and Kao–PEMAs at 400°C in Fig. 11a, PMA forms more easily in Kao–PEMAs, and the formation of PMAn is slower in Kao–PEMA (THF). At 420°C, as can be seen in Fig. 11a, the decomposition of PMAn in Kao–PEMA (DEE:EtOH) occurs more rapidly than it does in THF.

As for Kao–PBMAs and PBMA, considerable differences were observed in their FTIR spectra at 350 and 400°C, as shown in Fig. 11b. At 350°C, the peak belonging to PMA was only observed in FTIR spectrum of Kao–PBMA (DCM). At 400°C, the peaks attributed to PMA and PMAn were observed at Kao–PBMAs400, but they did not appear in PBMA. However, the decomposition rate of PMAn in the FTIR spectra of Kao–PBMA prepared in DCM was higher than that of the one occurred in THF. The findings showed that kaolinite accelerated the formation of PMA and the decomposition of PMAn and that the acceleration effect was found to be greater in Kao–PBMA (DCM) than in Kao–PBMA (THF).

In regard to the FTIR spectra obtained for PCHMA300 and KaoPCHMA300, no significant difference was observed. Compared to the FTIR spectra of PIBOMA and Kao–PIBOMAs at 250 and 275°C, as shown in Fig. 11c, it can be seen that PMA was formed previously in Kao–PIBOMAs.

CONCLUSIONS

A comparative study was carried out to examine what kind of effects those three factors—solvent, clay structure, and the functional groups in the PaMAs—would have on the thermal properties of the PaMA materials with clay, through utilization of the relationships among their solubility parameters and of the probable interactions among PaMAs, clays, the modifier (ODA) and solvents.

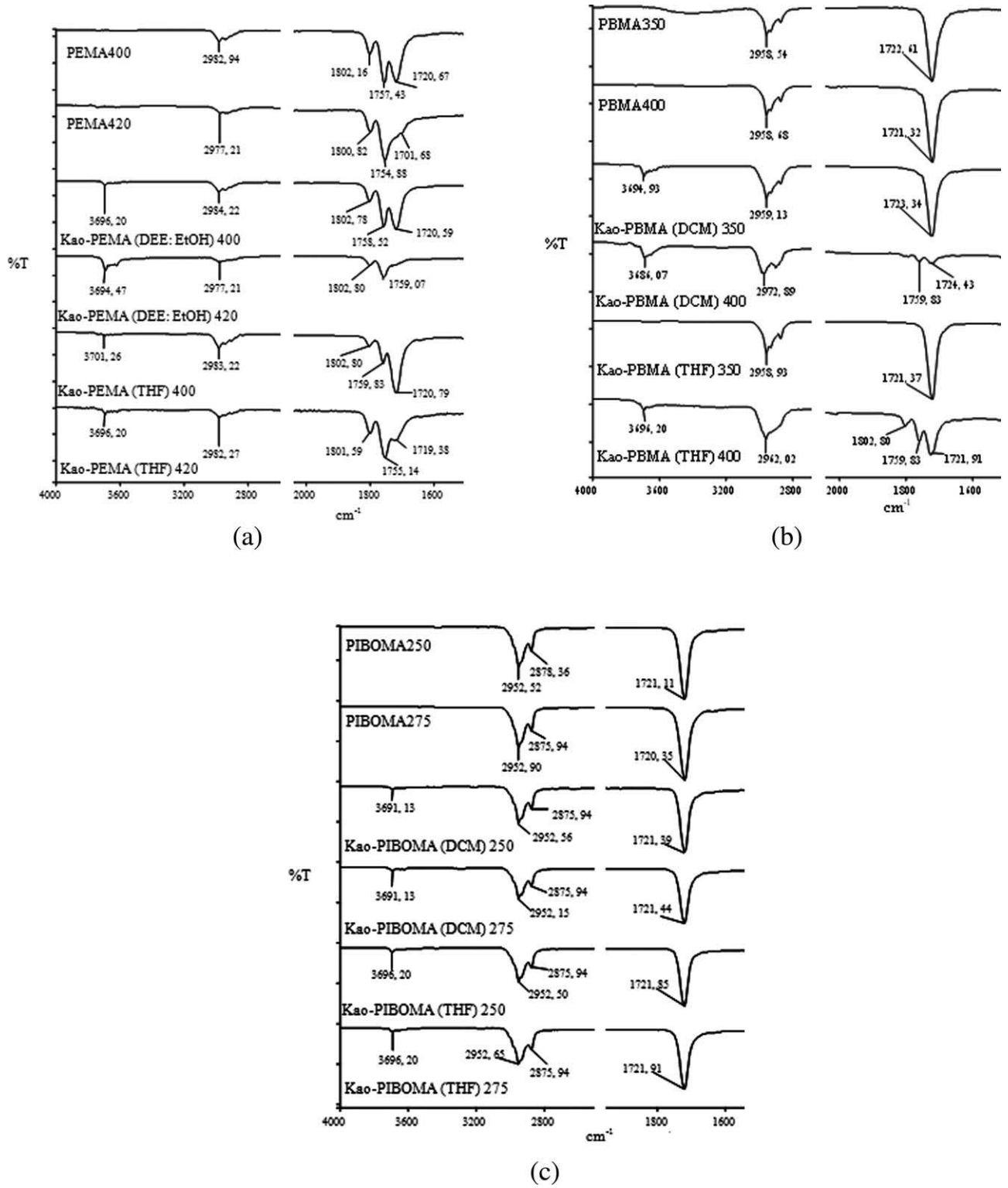

FIG. 11. (a) FTIR spectra for the residues of PEMA and Kao–PEMAs at 400 and 420°C. (b) FTIR spectra for the residues of PBMA and Kao–PBMAs at 350 and 400°C. (c) FTIR spectra for the residues of PIBOMA and Kao–PIBOMAs at 250 and 275°C.

The resultant materials can include exfoliated (I), intercalated (II), and undispersed (III) kaolinite depending on their XRD patterns. TEM micrographs also revealed that platy and tube structures of kaolinite and their stacked form would disperse the PaMAs. Therefore, these materials were called PaMAs–kaolinite materials with mixed morphology. The thermal stabilities of these structures are observed to be in the order of I > II and/or III and II > III. The fact

 DOI 10.1002/pc

that the increase was observed even in the thermal stability of the materials involving the third structure shows that exfoliation has occurred even if only to a small degree.

The type of solvent affects the thermal stability and the glass transition temperature of the PaMAs. THF can be the most suitable solvent for increasing thermal stability of the PaMAs in the presence of the kaolinite, as used in this study, due to the closeness of solubility parameters of ODA and THF and due to the change of 3D solubility parameters of kaolinite after its modification with ODA. The fact that THF is cyclic ether and thus has an oxygen atom with unpaired electrons can also facilitate the interaction between the PaMAs and Kao–Int. In addition, Kao–Int could increase more in T_g of PaMAs with a lower f_d and higher f_h in THF medium.

When comparing the thermal stabilities of Kao–PaMAs (THF) and the change in f_d and f_h of linear PaMAs, a higher dispersion force and a lower hydrogen-bonding force of the PaMAs facilitate the dispersion of Kao–Int in them and cause better thermal stability of the Kao–PaMAs materials. The result is consistent with the finding that the interaction among PaMA, THF, and Kao–Int improves when occurred from PMMA to PEMA and PBMA. The fact that the materials of the linear PaMAs with kaolinite have better thermal stability than those of the ring PaMAs in THF medium shows that Kao–Int is not dispersed well in the ring PaMAs. This could result from the fact that the bulky ester groups in the ring PaMAs cause the steric effect and that this effect hampers the interaction between COO^- group in the PaMAs and Kao–Int. The closeness of the solubility parameters of the ring PaMAs and of the solvents could not explain the results obtained for them. Owing to the fact that the polymers with aromatic rings all show rather restricted solubility ranges, Kao–PBzMA could have less thermal stability. No more accurate explanation for the changes in their thermal stability could be made due to the lack of 3D solubility parameters of the PaMAs in the literature.

The obtained results relating to the thermal stability of Kao–PaMAs prepared in different solvents show that it is necessary to balance $\delta_{d,}$ δ_p, and δ_h components of solvents and PaMAs. PaMAs with higher f_d and f_p and less f_h disperse usually well in solvents/mixture with higher f_h in the presence of Kao–Int and vice versa.

Even though kaolinite was not as easily dispersed as sepiolite in PEMA and PHEMA depending on their XRD patterns, the fact that Kao–PEMA/PHEMA materials have better thermal stability than Sep–PEMA/PHEMA and that DEE:EtOH and EtOH provide better thermal stability to Sep–PaMAs than Kao–PaMAs can stem from the δh component difference between sepiolite and Kao–Int. On the other hand, PaMAs with higher or lower f_h disperse well in solvents with higher f_h in the presence of sepiolite and the f_h parameter of the solvent/mixture facilitating the dispersion of sepiolite in the PaMAs is higher than that of Kao–Int.

When the change in T_g temperatures of PaMAs in the presence of Kao–Int/sepiolite was compared to the relationship between the solubility parameters of PaMAs and solvents, it was found that a solvent/mixture with higher f_h usually caused an increase in T_g temperatures of PaMAs materials.

Also, kaolinite and the type of solvent usually have an effect on the formation/decomposition of PMA and PMAn in degradation mechanism of PaMAs. For Kao–PEMAs and Kao–PHEMAs, the effect is usually similar to the change caused by sepiolite in the degradation mechanism of PEMA and PHEMA.

The attempts to explain the relationship between solubility parameters and thermal properties of Kao–PaMAs show that using the Hildebrand solubility parameters is more suitable to explain only the compatibility between modifier/modified clay and solvent, while the compatibility among polymer/polymer type, fillers, and solvents can be explained accurately by using the Hansen solubility parameters/spheres.

ACKNOWLEDGMENTS

The authors thank Prof. İsmet Kaya for DSC measurements.

REFERENCES

1. L. Benco, D. Tunega, J. Hafner, and H. Lischka, *J. Phys. Chem. B*, **105**, 10812 (2001).
2. A. Ammala, A.J. Hill, K.A. Lawrence, and T. Tran, *J. Appl. Polym. Sci.*, **104**, 1377 (2007).
3. T.J. Pinnavaia and G.W. Beal, *Polymer-Clay Nanocomposites*, Wiley, England (2000).
4. X. Jia, Y. Li, B. Zhang, Q. Cheng, and S. Zhang, *Mater. Res. Bull.*, **43**, 611 (2008).
5. Y. Komori, Y. Sugahara, and K. Kuroda, *Chem. Mater.*, **11**, 3 (1999).
6. T. Itagaki, A. Matsumura, M. Kato, A. Usuki, and K. Kuroda, *J. Mater. Sci. Lett.*, **20**, 1483 (2001).
7. H.A. Essawy, *Colloid. Polym. Sci.*, **286**, 795 (2008).
8. Y. Li, B. Zhang, and X. Pan, *Compos. Sci. Technol.*, **68**, 1954 (2008).
9. Z. Chen, C. Huang, S. Liu, Y. Zhang, and K. Gong, *J. Appl. Polym. Sci.*, **75**, 796 (2000).
10. L. Cabedo, E. Gimenez, J.M. Lafaron, R. Gavara, and J.J. Saura, *Polymer*, **45**, 5233 (2004).
11. H.A. Essawy, A.M. Youssef, and A.A. Abd El-Hakim, *Polym. Plast. Technol. Eng.*, **48**, 177 (2009).
12. Y. Turhan, M. Dŏgan, and M. Alkan, *Ind. Eng. Chem. Res.*, **49**, 1503 (2010).
13. J.L. Capiteno, F.T. da Silva, and V.R. Caffarena, "Preparation of Layered Polyvinyl Chloride (PVC)-Kaolinite Nanocomposites," http://www.icam2004.org/upload/pap0114.pdf (26.01.06), 2004 ICAM-BR, São Paulo.
14. K. Fukushima, D. Tabuani, and G. Camino, *Mater. Sci. Eng. C*, **29**, 1433 (2009).

15. S. Xie, S. Zhang, F. Wang, M. Yang, R. Seguela, and J.-M. Lefebvre, *Comp. Sci. Technol.*, **67**, 2334 (2007).
16. L. Bokobza, *J. Appl. Polym. Sci.*, **93**, 2095 (2004).
17. M. Alkan and R. Benlikaya, *J. Appl. Polym. Sci.*, **112**, 3764 (2009).
18. Y. Li and H. Ishida, *Polymer*, **44**, 6571 (2003).
19. A. Choudhury, A.K. Bhowmick, and C. Ong, *Polymer*, **50**, 201 (2009).
20. Y.S. Choi, T.H. Ham, and I.J. Chung, *Chem. Mater.*, **16**, 2522 (2004).
21. D.L. Ho and C.J. Glinka, *Chem. Mater.*, **15**, 1309 (2003).
22. H. Ishida, S. Campbell, and J. Blackwell, *Chem. Mater.*, **12**, 1260 (2000).
23. F. Chavarria and D.R. Paul, *Polymer*, **45**, 8501 (2004).
24. R. Benlikaya, M. Alkan, and İ. Kaya, *Polym. Compos.*, **30**, 1585 (2009).
25. B.N. Jang, D. Wang, and C.A. Wilkie, *Macromolecules*, **38**, 6533 (2005).
26. M. Alkan, C. Hopa, Z. Yilmaz, and H. Guler, *Micropor. Mesopor. Mater.*, **86**, 176 (2005).
27. Y. Komori, Y. Sugahara, and K. Kuroda, *Appl. Clay Sci.*, **15**, 241 (1999).
28. Z. Shen, G.P. Simon, and Y.B. Cheng, *Polymer*, **43**, 4251 (2002).
29. Y. Liang, Y. Wang, Y. Wu, Y. Lu, H. Zhang, and L. Zhang, *Polym. Test.*, **24**, 12 (2004).
30. J.J. Tuney and C. Detellier, *Chem. Mater.*, **8**, 927 (1996).
31. Y. Komori, H. Enoto, R. Takenawa, S. Hayashi, Y. Sugahara, and K. Kuroda, *Langmuir*, **16**, 5506 (2000).
32. J.L. Acosta, L. Gonzáles, M.C. Ojeda, and C.D. Rio, *J. Appl. Polym. Sci.*, **86**, 3512 (2002).
33. J.E. Gardolinski, L.C.M. Carrera, M.P. Cantao, and F. Wypych, *J. Mater. Sci.*, **35**, 3113 (2000).
34. E. Duquesne, S. Moins, M. Alexandre, and P. Dubois, *Macromol. Chem. Phys.*, **208**, 2542 (2007).
35. T. Lindvig, M.L. Michelsen, and G.M. Kontogeorgis, *Fluid Phase Equilibr.*, **203**, 247 (2002).
36. J. Burke, *The Oakland Museum of California August 1984, Appeared in the AIC Book and Paper Group Annual, Vol. 3* (1984). Available at: http://cool.conservation-us.org/byauth/burke/solpar/solpar6.html
37. R. W. Richards, *Polymer*, **18**, 114 (1977).
38. İ. Kaya and E. Özdemir, *Polymer*, **40**, 2405 (1999).
39. A. Mu'gica, J.A. Pomposo, E. Calahorra, and M. Cortázar, *Polymer*, **46**, 10741 (2005).
40. http://www.stenutz.eu/chem/solv24.php?sort=3i.
41. J.N. Coleman, *Adv. Funct. Mater.*, **19**, 3680 (2009).
42. R.B. Romero, C.A.P. Leite, and M.d.C. Gonçalves, *Polymer*, **50**, 161 (2005).
43. A. Lafaurie, N. Azema, L. Ferry, and J.-M. Lopez-Cuesta, *Powder Technol.*, **192**, 92 (2009).
44. P. Slobodian, A. Lengálová, P. Sáha, and M. Slouf, *J. Reinf. Plast. Comp.*, **26**, 1705 (2007).
45. L.J. Hughes and G.E. Britt, *J. Appl. Polym. Sci.*, **15**, 337 (1961).
46. M. Coskun, K. Demirelli, I. Erol, and M. Ahmedzade, *Polym. Degrad. Stab.*, **61**, 493 (1998).
47. F. Bertini, G. Audisio, and V.V. Zuev, *Polym. Degrad. Stab.*, **89**, 233 (2005).

 DOI 10.1002/pc